FULL PAPER

Ruthenium Complexes of Easily Accessible Tridentate Ligands Based on the 2-Aryl-4,6-bis(2-pyridyl)-s-triazine Motif: Absorption Spectra, Luminescence Properties, and Redox Behavior

Matthew I. J. Polson,[a] Elaine A. Medlycott,[a] Garry S. Hanan,*[a] Larisa Mikelsons,[b] Nick J. Taylor,[b] Masashi Watanabe,[c] Yasutaka Tanaka,[c] Frédérique Loiseau,*[d] Rosalba Passalacqua,[d] and Sebastiano Campagna[d]

Dedicated to Professor Jean-Marie Lehn on the occasion of his 65th birthday

Abstract: A family of tridentate ligands **1a–e**, based on the 2-aryl-4,6-di(2-pyridyl)-s-triazine motif, was prepared along with their hetero- and homoleptic Ru^{II} complexes **2a–e** ([Ru(tpy)(**1a–e**)]$^{2+}$; tpy=2,2′:6′,2′′-terpyridine) and **3a–e** ([(Ru(**1a–e**)$_2$]$^{2+}$), respectively. The ligands and their complexes were characterized by ^{1}H NMR spectroscopy, ES-MS, and elemental analysis. Single-crystal X-ray analysis of **2a** and **2e** demonstrated that the triazine core is nearly coplanar with the non-coordinating ring, with dihedral angles of 1.2 and 18.6°, respectively. The redox behavior and electronic absorption and luminescence properties (both at room temperature in liquid acetonitrile and at 77 K in butyronitrile rigid matrix) were investigated. Each species undergoes one oxidation process centered on the metal ion, and several (three for **2a–e** and four for **3a–e**) reduction processes centered on the ligand orbitals. All compounds exhibit intense absorption bands in the UV region, assigned to spin-allowed ligand-centered (LC) transitions, and moderately intense spin-allowed metal-to-ligand charge-transfer (MLCT) absorption bands in the visible region. The compounds exhibit relatively intense emissions, originating from triplet MLCT levels, both at 77 K and at room temperature. The incorporation of triazine rings and the near planarity of the noncoordinating ring increase the luminescence lifetimes of the complexes by lowering the energy of the ^{3}MLCT state and creating a large energy gap to the dd state.

Keywords: ligand design · luminescence · N ligands · ruthenium · triazines

[a] Dr. M. I. J. Polson, E. A. Medlycott, Prof. Dr. G. S. Hanan
Département de Chimie, Université de Montréal
2900 Edouard Montpetit, Montréal, QC, H3T 1J4 (Canada)
Fax: (+1) 514-343-7586
E-mail: garry.hanan@umontreal.ca

[b] L. Mikelsons, Dr. N. J. Taylor
Department of Chemistry, University of Waterloo
200 University Ave., Waterloo, Ontario, N2L 3G1 (Canada)

[c] M. Watanabe, Prof. Dr. Y. Tanaka
Faculty of Engineering, Shizuoka University
Hamamatsu, 432-8561 (Japan)

[d] Dr. F. Loiseau, R. Passalacqua, Prof. Dr. S. Campagna
Dipartimento di Chimica Inorganica
Chimica Analitica e Chimica Fisica
Università di Messina, 98166 Messina (Italy)
Fax: (+39) 090-393756
E-mail: photochem@chem.unime.it

Introduction

Over the past two decades, ruthenium–polypyridyl complexes have attracted considerable attention due to their outstanding photophysical properties.[1] The prototypical [Ru(bpy)$_3$]$^{2+}$ (bpy=2,2′-bipyridine) and [Ru(tpy)$_2$]$^{2+}$ (tpy=2,2′:6′,2′′-terpyridine) complexes are stable to a wide range of oxidative and reductive conditions, and are also photostable under suitable experimental conditions. The [Ru(bpy)$_3$]$^{2+}$ motif has been studied more extensively due to its facile synthesis and superior photophysical properties as compared to [Ru(tpy)$_2$]$^{2+}$. These enhanced properties include a longer room-temperature (RT) excited-state lifetime, which is critical for applications in practical devices,[2] and a higher quantum yield. However, as the [Ru(bpy)$_3$]$^{2+}$ motif is stereogenic, polymetallic complexes based thereon will give rise to a complicated mixture of isomers.[3] On the other hand, the achiral [Ru(tpy)$_2$]$^{2+}$ motif has the advantage of forming unique polymetallic complexes when substituted in the 4′-position,[4] and thus simplifies synthesis. The short

RT excited-state lifetime of [Ru(tpy)$_2$]$^{2+}$ has also spurred efforts to develop RT luminescent analogues.[5] These efforts have met with limited success, usually requiring multistep syntheses or expensive starting materials.[6]

We recently reported a new strategy to improve RT luminescence in [Ru(tpy)$_2$] complexes by using a coplanar arrangement of aromatic substituents on the terpyridine ligand.[7] The idea was based on the observation that appropriately substituted heterocyclic rings lead to a coplanar arrangement of rings, as opposed to the slight twist found between aromatic hydrocarbon rings (Figure 1).[8] Coplanarity
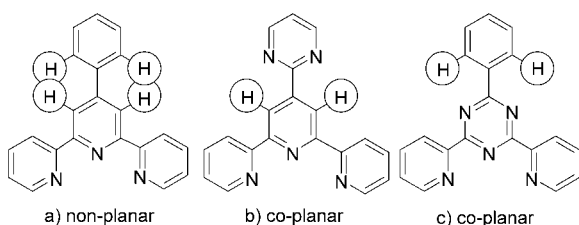

Figure 1. Coplanar and nonplanar arrangements of substituted terpyridines.

of heterocyclic rings has also been found to introduce interesting properties into ruthenium complexes of bidentate ligands,[9] including ion-sensing properties in diruthenium complexes.[10]

The improvement can be seen by comparing the RT excited-state lifetimes of Ru^{II} complexes of 4′-phenyl-tpy (0.5 ns, Figure 1a) and 4′-p-tolyl-tpy (0.95 ns) to the tpy analogue 4′-(2-pyrimidyl)-tpy (8 ns, (Figure 1b). The 4′-phenyl-tpy and 4′-p-tolyl-tpy ligands have unfavorable steric interactions between the H atoms adjacent to the interannular bond that cause twisting in the rings and less favorable π-orbital overlap between them as compared to 4′-(2-pyrimidyl)-tpy. In the last-named, coplanarity of the rings is achieved by substituting a series of functionalized 2-pyrimidyl groups in the 4′-position of tpy (Figure 1b). This arrangement allows the central and noncoordinating rings to undergo favorable C–H⋯N hydrogen bonding and thus lie coplanar with one another, which increases π-orbital overlap between the rings. Although the RT excited-state lifetimes of the Ru complexes of the substituted 4′-(2-pyrimidyl)-tpy are increased dramatically (up to 200 ns),[7] six steps are required to obtain these ligands from commercially available materials. A new approach to this strategy is to build up ligands with the additional N atoms on the central ring and not on the noncoordinating ring (Figure 1c). Although the synthesis and complexation of tris-substituted triazines have been described (e.g., tris-(2-pyrimidyl)-s-triazine[11] and tris-(2-pyridyl)-s-triazine[12]), almost no attention has been paid to the synthesis of unsymmetrically substituted tridentate ligands containing a central triazine ring. This stems in part from a relatively limited set of reaction conditions for building up the bis-(2-pyridyl)-s-triazine core of the ligands.[13] We recently presented a straightforward synthesis of unsymmetrically substituted tridentate triazine-based ligands and showed that their Ru complexes have interesting photophysical properties that include RT luminescence in liquid solution.[14]

Here we report the full synthetic details and properties of triazine-based tridentate ligands that exhibit improved RT excited-state lifetimes in their Ru^{II} complexes compared to the prototypes [Ru(tpy)$_2$]$^{2+}$ and [Ru(4′-phenyl-tpy)$_2$]$^{2+}$. Their inexpensive starting materials and superior photophysical properties make these new species ideal candidates for incorporation into larger supramolecular assemblies and devices.[15]

Results and Discussion

Synthesis and characterization: The three ligands with aromatic hydrocarbon rings, **1a–c**, were synthesised by treating two equivalents of 2-cyanopyridine with the lithium amidinide salt of the appropriate aromatic hydrocarbon in diethyl ether (Scheme 1). The amidinide salt was obtained in situ
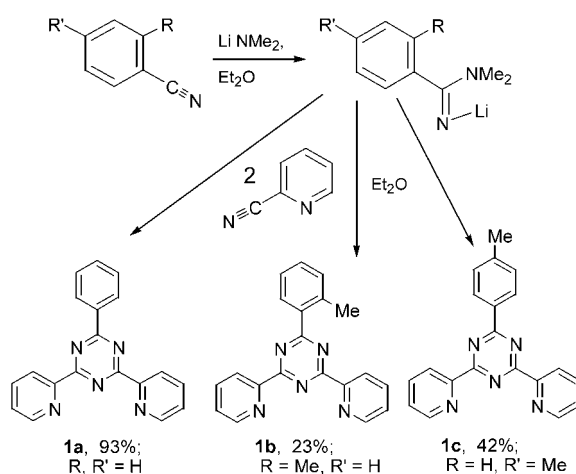
Scheme 1. Preparation of ligands **1a–c**.

from the appropriate aryl cyanide and lithium dimethylamide. Ligands **1a–c** were isolated from the reaction mixture by filtration and purified by recrystallization from EtOH/H$_2$O. The yield varied from 93% for unsubstituted **1a** to 23% for sterically encumbered *ortho*-methyl-substituted **1b**. The synthesis of **1a** is also possible in THF, albeit with a lower overall yield (70%).
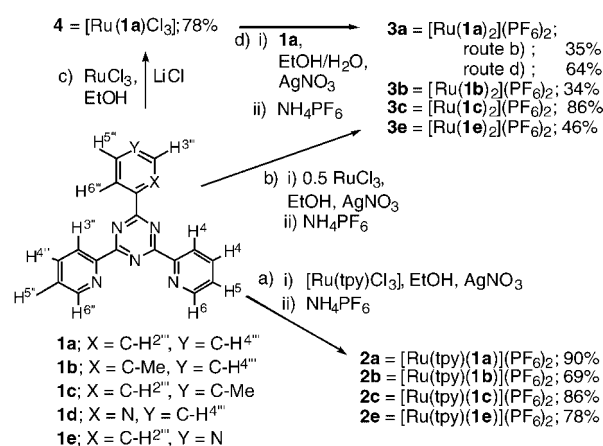
Under the same reaction conditions, heterocyclic cyanides failed to afford the desired ligands **1d,e**. Heterocyclic ligands **1d,e** could be obtained (Scheme 2) by modifying a literature procedure (**1d**) or by a statistical reaction based on the same procedure (**1e**). In both cases, two equivalents of 2-cyanopyridine were combined with one equivalent of 2-cyano- (**1d**) or 4-cyanopyridine (**1e**) and heated to 180°C in the presence of a catalytic amount of NaH. In the case of **1d**, the solid mass was extracted with toluene, and the resulting solid recrystallized from EtOH to afford **1d** in 67% yield. In the synthesis of **1e**, the resulting solid was treated with aqueous NiCl$_2$ after toluene extraction.[16] NiCl$_2$ forms a complex with **1e** and any **1d** that formed due to the statistical nature of the reaction. The aqueous phase was then extracted with dichloromethane to remove any bis- or tris(4-pyridyl)triazine formed during the reaction, and after de-
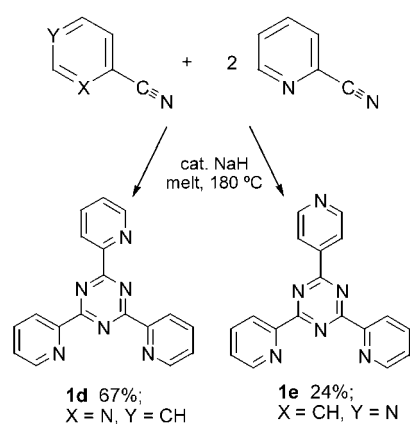
Scheme 2. Preparation of ligands **1d,e**.

Scheme 3. Preparation of ruthenium complexes **2** and **3**.

complexation of the Ni complexes with CN⁻, ligands **1d** and **1e** were collected and separated by recrystallization to afford **1e** in 24% yield.

Heteroleptic Ru complexes **2a–e** were synthesised by treating [Ru(tpy)Cl₃] with ligands **1** in the presence of AgNO₃ in EtOH/H₂O (Scheme 3a). The use of silver and an extended reaction time were critical for disfavoring the formation of two as-yet unidentified purple by-products. The complexes still required column chromatography to remove small amounts of these impurities. In the case of homoleptic complexes **3a–e**, the formation of purple impurities was unavoidable in the traditional one-step synthesis, even with an excess of silver (Scheme 3b). In a stepwise approach, preparation of trichlororuthenium(III) complex **4** (Scheme 3c) followed by synthesis of **3a** (Scheme 3d) gave an improved yield of 50% over two steps (vs 35%), as less purple by-products were formed.

Low-resolution electrospray mass spectrometry confirmed the molecular mass of complexes **2** and **3**, which ionize to their 1+ and 2+ species. In each case, the charge is associated with the successive loss of the PF_6^- counterions. Further confirmation of the purity of the metal complexes was afforded by elemental analysis. Hydrates of each complex were obtained, which is typical for ruthenium polypyridyl complexes.[17]

The ¹H NMR resonances for ligands **1** and complexes **2** and **3** are listed in Table 1, and the numbering scheme is given in Scheme 3. There is a pronounced shift in the ¹H NMR resonances of the ligand protons due to several factors that affect their chemical shifts on metal complexation. Firstly, the conformation of the pyridine N atoms changes from *transoid* to *cisoid* to permit metal chelation. As the nitrogen lone pairs deshield the ligand protons adjacent to the interannular bond in the *transoid* form of the ligands, metal complexation typically causes an upfield shift in their resonances in tpy complexes (cf. tpy and $[Ru(tpy)_2]^{2+}$ in Table 1). In the case of complexes **2** and **3**, the H³,³″ protons are forced into the plane of the central triazine ring, and this causes significant deshielding compared to $H^{T3,3″}$ on the tpy ligands in complexes **2** (Table 1). Secondly, the coordinated metal ion shifts the ligand proton resonances adjacent to the N atom upfield due to the magnetic anisotropy of the bound metal ion.[18] The H⁶,⁶″ protons of complexes **2** and **3** clearly follow this trend, although the

Table 1. ¹H NMR chemical shifts for ligands **1** and Ru complexes **2** and **3**.[a]

	3,3″	4,4″	5,5″	6,6″	2‴	3‴	4‴	5‴	6‴	Me	T3,3″	T4,4″	T5,5″	T6,6″	T3′	T4′
1a	8.75	7.89	7.47	8.90	8.75	7.51	7.56	7.51	8.75							
1b	8.75	7.93	7.50	8.92		7.43	7.43	7.43	8.26	2.79						
1c	8.80	7.94	7.51	8.93	8.69	7.36		7.36	8.69	2.46						
1d	8.77	7.88	7.46	8.90		8.77	7.88	7.46	8.90							
1e	8.79	7.95	7.53	8.91	8.85	8.56		8.56	8.85							
tpy											8.62	7.86	7.33	8.70	8.46	7.96
$[Ru(tpy)_2]^{2+}$											8.50	7.42	7.17	7.34	8.76	8.42
2a	9.06	8.11	7.40	7.57	9.06	7.83	7.83	7.83	9.06		8.50	7.91	7.11	7.44	8.78	8.46
2b	8.98	8.08	7.39	7.55		7.69	7.69	7.69	8.75	3.12	8.50	7.92	7.13	7.46	8.77	8.45
2c	9.04	8.09	7.38	7.54	8.94	7.62		7.62	8.94	2.57	8.48	7.91	7.10	7.44	8.77	8.45
2d	9.02	8.11	7.42	7.59		9.05	8.23	7.77	9.12		8.50	7.91	7.10	7.41	8.79	8.48
2e	9.10	8.13	7.41	7.59	9.05	8.85		8.85	9.05		8.50	7.91	7.10	7.43	8.79	8.49
3a	9.10	8.13	7.38	7.71	9.10	7.85	7.85	7.85	9.10							
3b	9.00	8.10	7.38	7.72		7.64	7.64	7.64	8.78	3.14						
3c	9.07	8.11	7.36	7.67	8.96	7.63		7.63	8.96	2.59						
3d	9.06	8.13	7.39	7.73		9.06	8.25	7.79	9.15							
3e	9.14	8.15	7.41	7.71	9.08	8.87		8.87	9.08							

[a] Ligands **1** and tpy in CDCl₃, and complexes **2–3** and $[Ru(tpy)_2]^{2+}$ in CD₃CN; see Scheme 3 for numbering scheme. tpy is assigned in an analogous way to ligands **1** and has the additional prefix T.

$H^{5,5''}$ protons show only a very slight shielding effect due to metal complexation.

The perpendicular arrangement of the ligands also affects the proton resonances in complexes **2** and **3**. The location of the protons *ortho* to the N atom in the peripheral pyridine rings ($H^{6,6'}$ and $H^{T6,6''}$) above the central heterocycle of the orthogonal ligand causes a significant upfield shift due to a ring-current effect. The proton *para* to the N atom in the central tpy pyridine ring ($H^{T4'}$) is held in the deshielding plane of the two terminal pyridine rings of ligands **1**. Both of these factors have previously been used as a measure of interligand shielding effects.[19] The external terpyridine resonances ($H^{T3–T6}$ and $H^{T3–T5'}$) are all within 0.05 ppm of each other; this indicates almost no difference in their local environments.

Variations in the solution concentrations of the ligands and complexes had very little effect on the chemical shifts of the protons, except in one particular case. Parent ligand **1a**, exhibited large shifts in its proton resonances on dilution from 10^{-3} to 10^{-5} M (Figure 2). Chemical shift changes of up
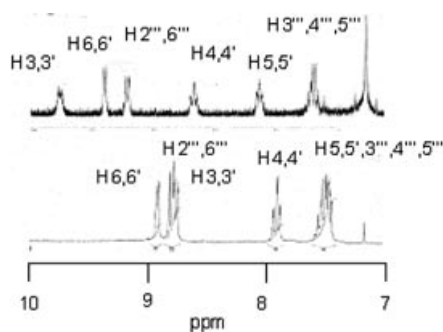
Figure 2. ^1H NMR spectra of ligand **1a** at low (top, 5×10^{-5} M) and high (bottom, 5×10^{-3} M) concentration in CDCl₃.

to 0.9 ppm were observed, and every proton resonance was affected. The other ligands in this family displayed shifts of less than 0.1 ppm on similar dilution. A possible explanation is that the ligand can effectively dimerize by noncovalent interactions at higher concentrations, whereby the relatively electron-rich phenyl group associates with the electron-poor triazine ring. Although several attempts were made to demonstrate potential dimerization by ES-MS, a molecular ion for twice the molecular mass of ligand **1a** was not observed.

Crystal structure determination of [2a](PF₆)₂ and [2e](PF₆)₂[20]: The X-ray crystal structure of heteroleptic ruthenium complex **2a** (Figure 3, top) contains mutually orthogonal tpy and **1a** ligands. The pseudo-octahedral geometry around the metal ion is similar to that of [Ru(tpy)₂]²⁺.[21] The Ru–N bond length (central triazine N) of 1.9648(16) Å is similar to that of 1.9824(16) Å for the central pyridine N atom in the tpy moiety. The phenyl ring in ligand **1a** is twisted by 1.2° relative to the central triazine ring. The dihedral angle N4-C7-C14-C15 is smaller than that found in any ruthenium 4′-phenyl-2,2′:6′,2″-tpy complex.[22] In the case of **2a**, there are no unfavorable H–H interactions *ortho* to the interannular bond, and the triazine N lone pairs are availa-
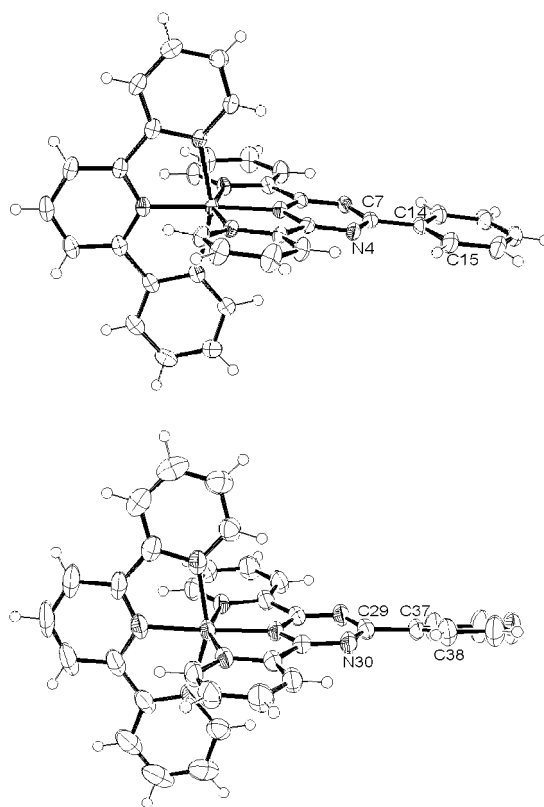
Figure 3. ORTEP representations of the X-ray crystal structures of complexes **2a** (top) and **2e** (bottom). The PF₆ counteranions have been omitted for clarity.

ble for hydrogen bonding to the C–H bonds on the phenyl substituent of **1a**. This also has consequences for the electro- and photochemistry of complexes **2** and **3** (vide infra).

The X-ray crystal structure of heteroleptic ruthenium complex **2e** (Figure 3, bottom) contains mutually orthogonal tpy and **1e** ligands in a pseudo-octahedral geometry around the metal ion. The Ru–N bond length to the triazine ligand of 1.965(2) Å is identical to that of **2a** and slightly shorter than the Ru–N bond length to the tpy ligand (1.989(2) Å). The pyridine ring is twisted by 17.6° relative to the central triazine ring. The twist in the dihedral angle (N30-C29-C37-C38) appears to occur in spite of the favorable C–H to N attraction between the triazine ring and the 4-pyridyl group. In addition, crystal-packing forces do not appear to be the cause, as no close contacts are noted in the extended solid-state structure of **2e**.

Electrochemistry: The electrochemistry of complexes **2** and **3** was studied in acetonitrile versus TBAPF₆ with ferrocene as internal standard. The data are gathered in Table 2, along with reported values for [Ru(tpy)₂]²⁺ as a model.

All the compounds exhibit one one-electron reversible oxidation process, except **3e**, which undergoes an irreversible oxidation, and three (**2a–e**) or four (**3a–e**) one-electron reversible reduction processes. The oxidation processes are ascribed to oxidation of the metal centers, as found for other Ru^{II}–polypyridyl complexes,[1,23] whereas the reduction processes are all centered on the ligand orbitals.

Table 2. Electrochemical redox potentials [V] (ΔE_p) for ligands **1** and complexes **2** and **3** in argon-purged acetonitrile.[a]

	Oxidation		Reductions		
1a	–	−1.50 (60)	–	–	–
1b	–	−1.51 (75)	–	–	–
1c	–	−1.51 (84)	–	–	–
1d	–	−1.44 (90)	–	–	–
1e	–	−1.36 (83)	–	–	–
2a	1.41 (82)	−0.77 (77)	−1.38 (66)	−1.64 (80)	–
2b	1.39 (78)	−0.78 (72)	−1.38 (69)	−1.64 (78)	–
2c	1.39 (82)	−0.78 (75)	−1.39 (89)	−1.64 (80)	–
2d	1.45 (93)	−0.74 (70)	−1.37 (76)	−1.62 (97)	–
2e	1.46 (94)	−0.69 (72)	−1.34 (70)	−1.59 (74)	–
3a	1.51 (81)	−0.71 (65)	−0.88 (69)	−1.51 (74)	−1.75 (78)
3b	1.50 (85)	−0.73 (70)	−0.90 (75)	−1.52 (76)	−1.77 (76)
3c	1.50 (101)	−0.74 (64)	−0.90 (70)	−1.53 (84)	−1.78 (87)
3d	1.60 (99)	−0.67 (66)	−0.86 (71)	−1.49 (97)	−1.75 (90)
3e	1.61 (irr)	−0.64 (56)	−0.82 (74)	−1.43 (81)	−1.69 (91)
[Ru(tpy)$_2$]$^{2+}$[b]	1.30	−1.24	−1.49		

[a] Versus SCE with ferrocene as internal standard. [b] From reference [25].

The oxidation potentials of all complexes are more positive than that of [Ru(tpy)$_2$]$^{2+}$ due to the stabilization of the metal-based orbitals by the triazine ring of ligands **1**. In a similar fashion, the Ru centers of homoleptic complexes **3a–e** are all more difficult to oxidize than those of heteroleptic complexes **2a–e** due to stabilization of the metal ion by the second triazine ring.

Comparison of the reduction potentials of heteroleptic complexes **2a–e** with those of [Ru(tpy)$_2$]$^{2+}$ (Table 2) is useful for attributing the processes to the various ligand orbitals. The first reduction waves of **2a–e** (around −0.75 V) occur at potentials much less negative than the first one of [Ru(tpy)$_2$]$^{2+}$. The first process can therefore be assigned to the reduction of the more electron deficient triazine-based ligand. Complexes **2a–e** undergo second reduction processes, one-electron and reversible, at slightly less negative potentials than the second reduction of [Ru(tpy)$_2$]$^{2+}$, and these are attributed to the reduction of the terpyridine ligand. The third reduction wave around −1.60 V is due to the second reduction process centered on the triazine-based ligand (e.g., Figure 4a).

The reduction pattern of the homoleptic complexes **3a–e**[24] shows four reduction processes, all reversible and one-electron (e.g., Figure 4b). The first two reduction waves can be attributed to successive reduction processes centered on the two triazine-based ligands. The first waves occur at slightly less negative potentials than those of complexes **2**, due to the presence of a second electron-deficient ligand **1** on the metal center. The second ligand becomes more difficult to reduce after addition of the first electron to the complex, that is, electronic communication between the ligands is efficient. The next two reduction waves, which present the same pattern as the first two (cf. the third reduction potentials of complexes **2a–e**), correspond to the second reduction processes of each of the two ligands. Interestingly, in the homoleptic complexes **3** (Table 2), the difference between the third and fourth reduction potentials (which is related to the interaction between the monoreduced ligands) is larger than the difference between first and second reduc-

tion potentials (which is related to the interaction between the not yet reduced ligands). For example, the third and fourth reduction processes of **3a** are separated by 240 mV, whereas the first and second reduction processes are separated by 170 mV (Table 2). This indicates that the interaction between the ligands is increased by reduction processes.

Electronic absorption spectra: The electronic absorption spectra of ligands **1** and their metal complexes **2** and **3** were measured in acetonitrile (Table 3). The electronic spectra of ligands **1** are dominated by moderately intense absorption bands near 240 and 275 nm attributed to π–π* transitions. Complexes **2** and **3** exhibit absorption spectra typical of Ru^{II}–polypyridine compounds,[1,2,26] characterized by ligand-centered π–π* transitions in the UV region and metal-to-ligand charge-transfer (MLCT) transitions in the visible part of the spectrum (Figure 5). Moreover, additional bands in the UV region near 300 and 330 nm are ascribed to the lower energy of triazine π–π* transitions as compared to terpyridine-based
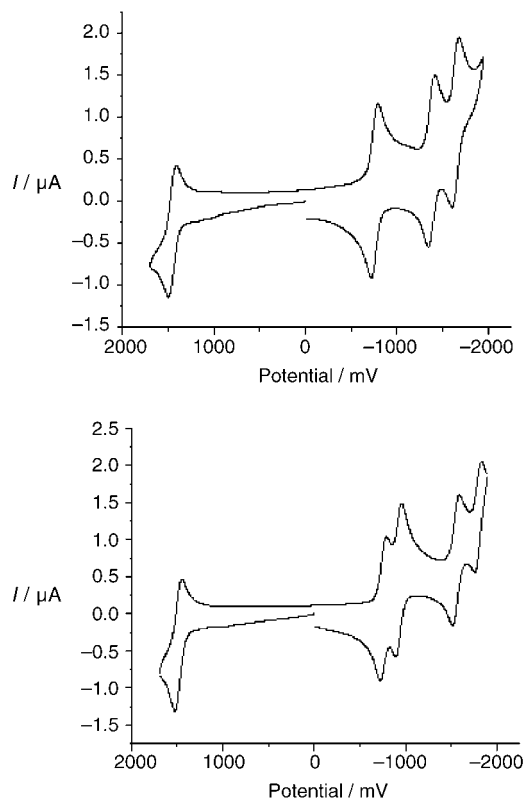

Figure 4. Cyclic voltammograms in acetonitrile with 0.1 M TBAPF$_6$ for complexes **2a** (top) and **3a** (bottom) at 100 mVs^{-1}.

Table 3. Electronic absorption maxima for ligands **1** and complexes **2** and **3**.[a]

	Wavelength λ_{max} [nm] (ε [10^3 cm^{-1} mol^{-1} dm^3]					
	¹MLCT		Ligand-centered π–π^* transitions			
1a			276 (40.8)			243 (25.0)
1b			280 (42.2)			244 (21.6)
1c			278 (40.4)			244 (25.0)
1d			278 (31.7)			244 (26.6)
1e			278 (28.5)			244 (37.1)
[Ru(tpy)₂][b]	474 (10.4)					
2a	515 (22.2)	332 (21.1)	299 (47.9)	279 (50.6)	272 (48.2)	242 (23.9)
	473 (17.7)					
2b	514 (12.1)	331 (25.3)	300 (53.1)	281 (53.8)	273 (53.3)	243 (27.7)
	470 (19.3)					
2c	519 (15.4)	331 (24.3)	302 (43.3)	281 (39.0)	272 (39.1)	243 (21.8)
	473 (16.9)					
2d	474 (19.6)[c]	331 (24.5)	299 (50.1)	280 (51.0)	273 (51.9)	242 (27.1)
2e	475 (17.6)[c]	331 (21.6)	298 (42.1)	282 (50.7)	273 (54.2)	243 (42.1)
3a	481 (24.6)			284 (73.2)		242 (24.4)
3b	474 (13.9)	329 (15.5)	291 (40.3)	277 (41.3)		243 (21.8)
3c	482 (17.8)	322 (34.4)	295 (40.8)	277 (43.1)		243 (19.2)
3d	500 (21.5)[c]	338 (15.5)	307 (43.5)	277 (65.4)		240 (28.6)
3e	508 (24.2)[c]	341 (15.3)	317 (36.0)	284 (82.9)		253 (33.7)

[a] In acetonitrile. [b] From reference [25]. [c] Broad.
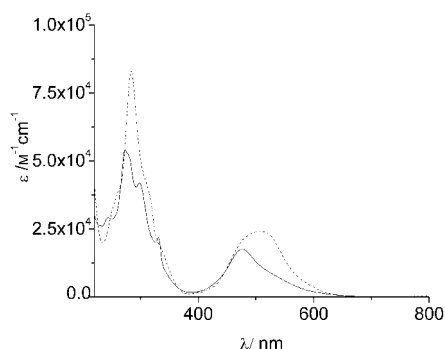
Figure 5. Absorption spectra for complexes **2e** (solid line) and **3e** (dotted line) in acetonitrile. Absorption maxima are given in Table 3.

complexes.[27] The MLCT absorption maxima of heteroleptic complexes **2** are very similar to that of [Ru(tpy)₂]²⁺ (Table 3) and are ascribed to a spin-allowed Ru-to-tpy MLCT transition. Each of complexes **2** has a lower energy absorption band (ca. 510–520 nm) which is ascribed to a spin-allowed Ru-to-**1** MLCT transition (Figure 5). The lower energy of these MLCT transitions is due to the low-lying π^* level of ligands **1**, as they contain an electron-deficient triazine ring.[28] The aryl substituent in the triazine 2-position also plays a role in lowering the energy of this band by extending the acceptor orbitals over an additional aromatic ring. The corresponding homoleptic complexes **3** all exhibit MLCT absorption bands at slightly higher energies with respect to the Ru-to-**1** MLCT

transition in compounds **2**, which is consistent with their having two triazine moieties per complex, as they stabilize the metal-based orbitals more than tpy does (cf. electrochemical data above). It is noteworthy that the highest energy Ru-to-**1** MLCT transitions occur in **2b** and **3b**. The aryl group is no longer coplanar with the triazine ring due to the *ortho*-methyl group, and this diminishes the size of the acceptor orbital.

Photophysics: Most of the complexes exhibit luminescence both at room temperature in liquid acetonitrile and at 77 K in butyronitrile rigid matrix. The photophysical data are gathered in Table 4, and the emission spectra of some of the compounds are shown in Figure 6. It is well known that the excited state responsible for the luminescence of Ru^{II}– polypyridine complexes is the lowest lying triplet MLCT excited state.[1,2,23] In heteroleptic compounds **2** and homoleptic complexes **3**, the emitting ³MLCT level involves the triazine-based ligand. At room temperature, the luminescence quantum yields are between one and two orders of magnitude higher than that of [Ru(tpy)₂]²⁺, and the excited state lifetimes are significantly longer (5–15 ns). For homoleptic complexes **3b** and **3c** having less electron withdrawing substituents on the triazine rings, no luminescence could be detected at room temperature, and the RT emission of compound **3d** was too weak to allow the measurement of its lifetime and quantum yield. In all the other cases in which luminescence was recorded, a significant red shift of the emission maximum was observed relative to that of [Ru(tpy)₂]²⁺, that is, additional nitrogen atoms on the central ring of the tridentate ligand stabilize the acceptor orbital of the MLCT excited state. Moreover, the presence of electron-withdrawing substituents on the triazine moiety further decreases the emission energy of the complexes. The emission energies of

Table 4. Photophysical data for complexes **2** and **3**.

	Luminescence, 298 K[a]					77 K[b]	
compound	λ_{max} [nm]	τ [ns]	ϕ	k_r [s^{-1}]	k_{nr} [s^{-1}]	λ_{max} [nm]	τ [µs]
2a	740	9	5×10^{-5}	5×10^3	11×10^7	695	1.1
2b	732	8	4×10^{-5}	5×10^3	12×10^7	685	1.1
2c	734	5	2×10^{-5}	3×10^3	20×10^7	679	1.4
2d	745	11	6×10^{-5}	5×10^3	9.1×10^7	700	1.0
2e	752	15	7×10^{-5}	4×10^3	6.7×10^7	707	1.3
3a	710	8	9×10^{-5}	11×10^3	1.2×10^7	672	1.4
3b						677	1.7
3c						667	1.6
3d	730					688	1.5
3e	722	4	10×10^{-6}	3×10^3	250.0×10^6	686	2.2
[Ru(tpy)₂]²⁺ [c]	629	0.25	$\leq 5 \times 10^{-6}$			598	10.6

[a] In deaerated CH₃CN. [b] In butyronitrile. [c] From reference [5].
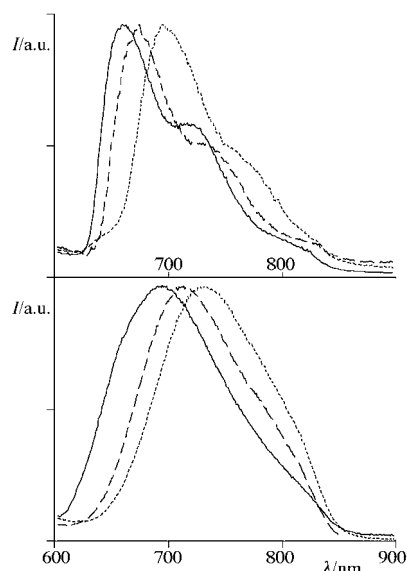
Figure 6. Normalized (uncorrected) emission spectra in liquid acetonitrile at room temperature (bottom) of **2b** (dashed line), **2e** (dotted line), and **3e** (solid line); and in butyronitrile rigid matrix at 77 K (top) of **2c** (dashed line), **2e** (dotted line), and **3c** (solid line). Corrected values of emission maxima are given in Table 4.

homoleptic complexes **3** are higher than those of heteroleptic complexes **2**; this is explained by the presence of a second triazine ring on the ruthenium center, which stabilizes the metal-centered orbital. Complex **2e** exhibits the longest excited-state lifetime (15 ns) as a result of the most electron accepting substituent on the triazine moiety, and this is the longest lifetime for a long-wavelength emission (>750 nm) in a $[Ru(tpy)_2]^{2+}$-type complex. As was previously observed for a series of analogous pyrimidyl–terpyridine-based Ru^{II} complexes (Figure 1b),[7] the compounds studied here do not obey the energy-gap law. Indeed, in the present complexes, as is common for Ru^{II} compounds containing tridentate polypyridine ligands, the main pathway for MLCT decay at RT is activated surface crossing to a higher lying metal-centered (MC) state.[1d, 2a, 7, 10] Red shift of emission energy (i.e., of the MLCT state) translates into a decreased efficiency of this thermally activated process (decreased k_{nr}), and therefore an increase in luminescence lifetime is obtained. Comparison with results obtained for pyrimidyl–terpyridine analogues of the type shown in Figure 1b indicates that enhancement of excited-state lifetimes is less efficient in the present case, most likely because the effect of enhanced delocalization in the acceptor ligand of the MLCT state, which is present in the pyrimidyl–terpyridine complexes, is less effective here, since the acceptor orbitals are mostly centered on the triazine ring. In a rigid matrix at 77 K, all the complexes are luminescent, with emission maxima again red-shifted relative to that of $[Ru(tpy)_2]^{2+}$, and exhibit longer excited-state lifetimes, on the microsecond timescale. In the case of complexes **2**, the emission energy decreases with increasing electron-withdrawing capacity of the substituent on the triazine ring, whereas in the case of homoleptic complexes this effect is less linear, due

to the stabilization of the metal orbitals by the presence of a second triazine-based ligand.

Conclusion

The synthetic procedures described here give ready access to a variety of aryl-substituted bis(2-pyridyl)-1,3,5-triazines. These tridentate ligands are excellent analogues of 2,2′:6′,2″-terpyridine, as they readily form transition metal complexes with a wide variety of metal ions. Both their homo- and heteroleptic ruthenium complexes display lower energy light absorption as compared to $[Ru(tpy)_2]^{2+}$. The concomitant decrease in the nonradiative decay pathways increases the room-temperature excited-state lifetimes of the complexes. All of the heteroleptic Ru^{II} complexes **2a–e** are luminescent at room temperature. Indeed, complexes **2a–e** have some of the longest lifetimes for monochromophoric excited states that emit beyond 730 nm. In the homoleptic series of Ru^{II} complexes, only complexes **3a** and **3e** have significant room-temperature excited-state lifetimes. The incorporation of triazine-based ligands **1a–e** into supramolecular assemblies by way of their RuCl$_3$ adducts (cf. **4**) may increase the room-temperature lifetime of the assemblies as compared to tpy or 4′-tolyl-2,2′:6′,2″-terpyridine analogues. We are currently exploring the synthetic versatility of ligands **1a–e** in assembling supramolecular arrays and will examine their photophysical properties.

Experimental Section

of exchanged electrons was measured by OSWV and by taking advantage of the presence of ferrocene used as the internal reference.

Experimental uncertainties: absorption maxima, ± 2 nm; molar absorption coefficient, 10; emission maxima, ± 5 nm; excited state lifetimes, 10%; luminescence quantum yields, 20%; redox potentials, ± 10 mV.

Compounds $\mathbf{1d}$,[32] $\mathbf{2d}$,[12b] $\mathbf{3d}$,[24] and [Ru(tpy)Cl₃][33] were synthesised as previously described. Solvents were removed under reduced pressure on a rotary evaporator unless otherwise stated.

Triazine ligands 1a–c: The corresponding aryl cyanide (3.84 mmol) was added to LiNMe₂ (200 mg) in diethyl ether (50 mL). After stirring for 30 min under nitrogen, 2-cyanopyridine was added (800 mg, 7.69 mmol). A precipitate formed rapidly and the resulting suspension was stirred overnight. The mixture was then poured into a 1:1 mixture of ethanol and water (200 mL). The solution was boiled on a hot plate to remove ethanol and diethyl ether. On cooling, a precipitate formed, which was collected by filtration.

Compound 1a: Yield 1.12 g (93%); ¹H NMR (CDCl₃, 300 MHz, TMS): $\delta = 8.90$ (d, $J = 4.5$ Hz, 2H; H$^{6,6'}$), 8.75 (m, 4H; H$^{3,3',2'',6''}$), 7.89 (t, $J = 7.5$ Hz, 2H; H$^{4,4''}$), 7.56 (t, $J = 7.0$ Hz, 1H; H$^{4''}$), 7.51 (t, $J = 7.5$ Hz, 2H; H$^{3'',5''}$), 7.47 ppm (dd, $J = 7.0, 5.0$ Hz, 2H; H$^{5,5'}$); MS (HREI): m/z: 311.1181 [M]⁺; elemental analysis calcd (%) for C₁₉H₁₃N₅: C 73.29, H 4.21, N 22.49; found: C 73.00, H 4.17, N 22.51.

Compound 1b: Yield 255 mg (23%); ¹H NMR (CDCl₃, 300 MHz, TMS): $\delta = 8.92$ (d, $J = 5.0$ Hz, 2H; H$^{6,6'}$), 8.75 (d, $J = 8.0$ Hz, 2H; H$^{3,3'}$), 8.26 (d, $J = 8.0$ Hz, 1H; H$^{6''}$), 7.93 (td, $J^t = 7.5$, $J^d = 1.5$ Hz, 2H; H$^{4,4'}$), 7.50 (ddd, $J = 7.5, 6.0, 1.0$ Hz, 2H; H$^{5,5'}$), 7.43 (dd, $J = 7.5, 1.5$ Hz, 1H; H$^{3''}$), 7.43 (m, 2H; H$^{4'',5''}$), 2.79 ppm (s, 3H; H^{Me}). MS (HREI): m/z: 325.1316 [M]⁺; elemental analysis calcd (%) for C₂₀H₁₅N₅·0.5 H₂O: C 71.84, H 4.82, N 20.94; found: C 71.73, H 4.42, N 21.03.

Compound 1c: Yield 468 mg (42%); ¹H NMR (CDCl₃, 300 MHz, TMS): $\delta = 8.93$ (d, $J = 4.0$ Hz, 2H; H$^{6,6'}$), 8.80 (d, $J = 8.0$ Hz, 2H; H$^{3,3'}$), 8.69 (d, $J = 8.0$ Hz, 2H; H$^{2'',6''}$), 7.94 (td, $J^t = 7.5$, $J^d = 1.5$ Hz, 2H; H$^{4,4''}$), 7.51 (dd, $J = 7.5, 5.0$ Hz, 2H; H$^{5,5''}$), 7.36 (d, $J = 8.0$ Hz, 2H; H$^{3'',5''}$), 2.46 ppm (s, 3H; H^{Me}). MS (HREI): m/z: 325.1328 [M]⁺; elemental analysis calcd (%) for C₂₀H₁₅N₅·H₂O: C 69.96, H 4.99, N 20.40; found: C 70.24, H 4.91, N 20.58.

Compound 1e: A mixture of 4-cyanopyridine (5 g), 2-cyanopyridine (5 g), and NaH (200 mg) was heated to 180 °C for 30 min. After cooling, the solid was dissolved in hot toluene (500 mL), and the solution filtered. While still hot, the toluene was extracted with an aqueous Ni solution (3 g of NiCl₂·6H₂O in 200 mL of water). After cooling, KCN (5 g) was added and a fine precipitate formed. The crude product was collected by filtration and recrystallized from ethanol. Yield 2.4 g (24%). ¹H NMR (CDCl₃, 300 MHz, TMS): $\delta = 8.91$ (d, $J = 3.5$ Hz, 2H; H$^{6,6'}$), 8.85 (d, $J = 5.5$ Hz, 4H; H$^{2'',6''}$), 8.79 (d, $J = 7.5$ Hz, 2H; H$^{3,3'}$), 8.56 (t, $J = 5.0$ Hz, 1H; H$^{3'',5''}$), 7.95 (t, $J = 7.5$ Hz, 2H; H$^{4,4''}$), 7.53 ppm (t, $J = 5.0$ Hz, 2H; H$^{5,5''}$); MS (HREI): m/z: 312.1123 [M]⁺; elemental analysis calcd (%) for C₁₈H₁₂N₆·0.5 H₂O: C 67.28, H 4.08, N 26.15; found: C 67.44, H 3.74, N 25.97.

Heteroleptic complexes 2a–e: The appropriate ligand (0.23 mmol) and AgNO₃ (115 mg, 0.68 mmol) were added to a suspension of [Ru(tpy)Cl₃] (100 mg, 0.23 mmol) in ethanol (50 mL). The mixture was then stirred and refluxed overnight. After cooling, the solution was filtered to remove AgCl and evaporated to dryness. The resulting solid was dissolved in acetonitrile and purified by column chromotography (SiO₂, acetonitrile/aq. KNO₃ 7:1). The nitrate salt was metathesized to the PF₆ salt, and the solvent removed under reduced pressure. The solid was dissolved in acetonitrile, and the product precipitated by addition to water.

Compound 2a: Yield 190 mg (90%); ¹H NMR (CD₃CN, 300 MHz, CD₂HCN); $\delta = 9.06$ (m, 4H; H$^{3,3',2'',6''}$), 8.78 (d, $J = 8.0$ Hz, 2H; T^{3,5}), 8.50 (d, $J = 7.5$ Hz, 2H; T$^{3,3'}$), 8.46 (t, $J = 8.0$ Hz, 1H; T^4), 8.11 (td, $J^t = 8.0$, $J^d = 1.0$ Hz, 2H; H$^{4,4'}$), 7.91 (td, $J^t = 7.0$, $J^d = 1.0$ Hz, 2H; T$^{4,4'}$), 7.83 (m, 3H; H$^{3'',4'',5''}$), 7.57 (d, $J = 5.5$ Hz, 2H; H$^{6,6''}$), 7.44 (d, $J = 5.5$ Hz, 2H; Hp$^{6,6''}$), 7.40 (td, $J^t = 5.5$, $J^d = 1.0$ Hz, 2H; H$^{5,5''}$), 7.11 ppm (t, $J = 6.0$ Hz, 2H; T$^{5,5''}$); MS (ESI): m/z: 791.4 [$M - \mathrm{PF_6}$]⁺, 323.5 [$M - 2\,\mathrm{PF_6}$]²⁺; elemental analysis calcd (%) for C₃₄H₃₂N₈RuP₂F₁₂·H₂O: C 42.55, H 3.21, N 11.90; found: C 42.53, H 2.91, N 12.39.

Compound 2b: Yield 152 mg (69%); ¹H NMR (CD₃CN, 300 MHz, CD₂HCN); 8.98 (d, $J = 7.5$ Hz, 2H; H$^{3,3''}$), 8.77 (d, $J = 8.0$ Hz, 2H; T^{3,5}),

8.75 (d, $J = 8.0$ Hz, 1H; H$^{5'''}$), 8.50 (d, $J = 8.5$ Hz, 2H; T$^{3,3'}$), 8.45 (t, $J = 8.5$ Hz, 1H; T^4), 8.08 (t, $J = 8.0$ Hz, 2H; H$^{4,4'}$), 7.92 (t, $J = 8.0$ Hz, 2H; T$^{4,4''}$), 7.69 (m, 3H; H$^{2''',3''',4'''}$), 7.55 (d, $J = 5.0$ Hz, 2H; H$^{6,6''}$), 7.46 (d, $J = 5.5$ Hz, 2H; T$^{6,6''}$), 7.39 (t, $J = 6.0$ Hz, 2H; T$^{5,5''}$), 7.13 (t, $J = 6.5$ Hz, 2H; T$^{5,5''}$), 3.12 ppm (s, 3H; CH₃); MS (ESI): m/z: 804.1 [$M - \mathrm{PF_6}$]⁺, 329.6 [$M - 2\,\mathrm{PF_6}$]²⁺; elemental analysis calcd (%) for C₃₅H₂₆N₈RuP₂F₁₂·H₂O: C 43.17, H 3.52, N 11.51; found: C 42.78, H 3.01, N 11.51.

Compound 2c: Yield 128 mg (86%); ¹H NMR (CD₃CN, 300 MHz, CD₂HCN); $\delta = 9.04$ (d, $J = 7.5$ Hz, 2H; H$^{3,3''}$), 8.94 (d, $J = 8.0$ Hz, 2H; H$^{2''',6''}$), 8.77 (d, $J = 8.0$ Hz, 2H; T$^{3',5'}$), 8.48 (d, $J = 8.5$ Hz, 2H; T$^{3,3'}$), 8.45 (t, $J = 8.5$ Hz, 1H; T^4), 8.09 (t, $J = 8.0$ Hz, 2H; H$^{4,4''}$), 7.91 (t, $J = 8.0$ Hz, 2H; T$^{4,4''}$), 7.62 (d, $J = 8.5$ Hz, 2H; H$^{3''',5'''}$), 7.54 (d, $J = 5.0$ Hz, 2H; H$^{6,6''}$), 7.44 (d, $J = 5.5$ Hz, 2H; T$^{6,6''}$), 7.38 (t, $J = 6.0$ Hz, 2H; H$^{5,5''}$), 7.10 (t, $J = 6.5$ Hz, 2H; T$^{5,5''}$), 2.57 ppm (s, 3H; CH₃); MS (ESI): m/z: 804.2 [$M - \mathrm{PF_6}$]⁺, 329.7 [$M - 2\,\mathrm{PF_6}$]²⁺; elemental analysis calcd (%) for C₃₅H₂₆N₈RuP₂F₁₂: C 43.99, H 3.38, N 11.72; found: C 43.85, H 3.01, N 11.47.

Compound 2e: Yield 165 mg (78%); ¹H NMR (CD₃CN, 300 MHz, CD₂HCN): $\delta = 9.10$ (m, $J = 8.0$ Hz, 2H; H$^{3,3''}$), 9.05 (m, 2H; H$^{2''',6''}$), 8.85 (d, $J = 7.5$ Hz, 2H; H$^{3''',5'''}$), 8.79 (d, $J = 8.0$ Hz, 2H; T^{3,5}), 8.50 (d, $J = 8.0$ Hz, 2H; T$^{3,3''}$), 8.49 (t, $J = 8.0$ Hz, 1H; T^4), 8.13 (td, $J^t = 8.0$, $J^d = 1.5$ Hz, 2H; H$^{4,4''}$), 7.91 (td, $J^t = 8.0$ Hz, $J^d = 1.0$ Hz, 2H; T$^{4,4''}$), 7.59 (d, $J = 5.0$ Hz, 2H; H$^{6,6''}$), 7.43 (d, $J = 5.5$ Hz, 2H; T$^{6,6''}$), 7.41 (d, $J = 5.5$ Hz, $J^d = 1.5$ Hz, 2H; H$^{5,5''}$), 7.10 ppm (td, $J^t = 6.0$ Hz, $J^d = 1.0$ Hz, 2H; T$^{5,5''}$); MS (ESI): m/z: 792.5 [$M - \mathrm{PF_6}$]⁺, 323.9 [$M - 2\,\mathrm{PF_6}$]²⁺; elemental analysis calcd (%) for C₃₃H₂₃N₉RuP₂F₁₂·H₂O: C 41.52, H 2.64, N 13.21; found: C 41.92, H 2.94, N 13.16.

Homoleptic complexes 3a–e: The appropriate ligand (0.64 mmol) and AgNO₃ (160 mg, 0.96 mmol) were added to a solution of RuCl₃·xH₂O (76 mg, 0.32 mmol) in ethanol (50 mL). The mixture was then stirred and refluxed overnight. After cooling, the solution was filtered to remove AgCl and evaporated to dryness. The resulting solid was dissolved in acetonitrile and purified by column chromotography (SiO₂, acetonitrile/aq. KNO₃ 7:1). The nitrate salt was metathesized to the PF₆ salt, and the solvent removed under reduced pressure. The solid was dissolved in acetonitrile, and the product precipitated by addition to water.

Compound 3a: Yield 105 mg (35%); ¹H NMR (CD₃CN, 300 MHz, CD₂HCN); $\delta = 9.10$ (m, 8H; H$^{3,3',2'',6''}$), 8.13 (td, $J^t = 8.0$ Hz, $J^d = 1.0$ Hz, 4H; H$^{4,4''}$), 7.85 (m, 6H; H$^{3''',4''',5'''}$), 7.71 (d, $J = 5.5$ Hz, 4H; H$^{6,6''}$), 7.38 ppm (td, $J^t = 7.5$ Hz, $J^d = 1.5$ Hz, 4H; H$^{5,5''}$); MS (ESI): m/z: 868.3 [$M - \mathrm{PF_6}$]⁺, 361.9 [$M - 2\,\mathrm{PF_6}$]²⁺; elemental analysis calcd (%) for C₃₈H₃₄N₁₀RuP₂F₁₂·H₂O: C 43.98, H 2.30, N 13.49; found: C 43.87, H 2.69, N 13.51.

Compound 3b: Yield 115 mg (34%); ¹H NMR (CD₃CN, 300 MHz, CD₂HCN); $\delta = 9.00$ (d, $J = 7.5$ Hz, 4H; H$^{3,3'}$), 8.78 (d, $J = 7.0$ Hz, 2H; H$^{5'''}$), 8.10 (t, $J = 7.5$ Hz, 4H; H$^{4,4'}$), 7.72 (d, $J = 5.5$ Hz, 4H; H$^{6,6''}$), 7.64 (m, 6H; H$^{2''',3''',4'''}$), 7.38 (t, $J = 6.5$ Hz, 4H; H$^{5,5''}$), 3.14 ppm (s, 6H; H^{Me}); MS (ESI): m/z: 895.8 [$M - \mathrm{PF_6}$]⁺, 375.8 [$M - 2\,\mathrm{PF_6}$]²⁺.

Compound 3c: Yield 99 mg (86%); ¹H NMR (CD₃CN, 300 MHz, CD₂HCN); $\delta = 9.07$ (d, $J = 8.0$ Hz, 4H; H$^{3,3'}$), 8.96 (d, $J = 8.0$ Hz, 4H; H$^{2'',6''}$), 8.11 (t, $J = 7.5$ Hz, 4H; H$^{4,4''}$), 7.67 (d, $J = 5.5$ Hz, 4H; H$^{6,6''}$), 7.63 (d, $J = 8.5$ Hz, 4H; H$^{3''',5'''}$), 7.36 (t, $J = 6.5$ Hz, 4H; H$^{5,5''}$), 2.59 ppm (s, 6H; CH₃); MS (ESI): m/z: 376.5 [$M - 2\,\mathrm{PF_6}$]²⁺.

Compound 3e: Yield 150 mg (46%); ¹H NMR (CD₃CN, 300 MHz, CD₂HCN); $\delta = 9.14$ (d, $J = 7.5$ Hz, 4H; H$^{3,3'}$), 9.08 (d, $J = 4.5$ Hz, 4H; H$^{2'',6''}$), 8.87 (d, $J = 4.5$ Hz, 4H; H$^{3''',5'''}$), 8.15 (t, $J = 8.0$ Hz, 4H; H$^{4,4''}$), 7.71 (d, $J = 5.0$ Hz, 4H; H$^{6,6''}$), 7.41 ppm (t, $J = 7.5$ Hz, 4H; H$^{5,5''}$); MS (ESI): m/z: 1017.3 [$M + \mathrm{H}$]⁺, 871.5 [$M - \mathrm{PF_6}$]⁺, 363.4 [$M - 2\,\mathrm{PF_6}$]²⁺; elemental analysis calcd (%) for C₃₆H₂₄N₁₂RuP₂F₁₂·H₂O: C 41.83, H 2.54, N 16.26; found: C 41.84, H 2.76, N 16.16.

Compound 4: Lithium chloride (4 g) was dissolved in ethanol (50 mL) with sonication. To this solution were added **1a** (1 g) and RuCl₃·xH₂O (770 mg). The solution was refluxed overnight and was continuously stirred by magnetic stirrer. On cooling the fine brown precipitate was collected by filtration. This crude product was suspended in ethanol, sonicated for 30 min, collected by filtration, and the process repeated. Yield 1.3 g (78%); elemental analysis calcd (%) for C₁₉H₁₃Cl₃N₅Ru·3 H₂O: C 39.84, H 3.34, N 12.23; found: C 38.50, H 2.59, N 11.88.

Compound 3a: Compound **1a** (0.32 mmol) and AgNO₃ (160 mg, 0.96 mmol) were added to a suspension of **4** (100 mg, 0.32 mmol) in ethanol (50 mL). The mixture was then stirred and refluxed overnight. After

cooling, the solution was filtered to remove AgCl and then evaporated to dryness. The resulting solid was dissolved in acetonitrile and purified by column chromatography (SiO$_2$, acetonitrile/aq. KNO$_3$ 7:1). The nitrate salt was metathesized to the PF$_6$ salt, and the solvent removed under reduced pressure. The solid was dissolved in acetonitrile, and the product was precipitated by addition to water. Yield 125 mg (64 %); physical data agreed with those given above.

Acknowledgement

[1] a) V. Balzani, A. Juris, M. Venturi, S. Campagna, G. Denti, S. Serroni, *Chem. Rev.* **1996**, *96*, 759; b) V. Balzani, F. Scandola, *Supramolecular Photochemistry*, Horwood, Chicester (UK), **1991**; c) J.-P. Sauvage, J.-P. Collin, J.-C. Chambron, S. Guillerez, C. Coudret, V. Balzani, F. Barigelletti, L. De Cola, L. Flamigni, *Chem. Rev.* **1994**, *94*, 993; d) T. J. Meyer, *Pure Appl. Chem.* **1986**, *58*, 1193, and references therein.

[2] a) A. Juris, V. Balzani, F. Barigelletti, S. Campagna, P. Belser, A. Von Zelewsky, *Coord. Chem. Rev.* **1988**, *84*, 85; b) L. Sun, L. Hammarström, B. Akermark, S. Styring, *Chem. Soc. Rev.* **2001**, *30*, 36; c) F. Barigelletti, L. Flamigni, *Chem. Soc. Rev.* **2000**, *29*, 1; d) A. Hagfeldt, M. Graetzel, *Acc. Chem. Res.* **2000**, *33*, 269; e) S. Encinas, L. Flamigni, F. Barigelletti, E. C. Constable, C. E. Housecroft, E. R. Schofield, E. Figgemeier, D. Fenske, M. Neuburger, J. G. Vos, M. Zehnder, *Chem. Eur. J.* **2002**, *8*, 137; f) D. S. Tyson, C. R. Luman, X. Zhou, F. N. Castellano, *Inorg. Chem.* **2001**, *40*, 4063.

[3] a) F. M. MacDonnell, M. D. M. Ali, M. J. Kim, *Comments Inorg. Chem.* **2000**, *22*, 203; b) A. von Zelewsky, O. Mamula, *J. Chem. Soc. Dalton Trans.* **2000**, 219.

[4] E. C. Constable, P. Harverson, C. E. Housecroft, *J. Chem. Soc. Dalton Trans.* **1999**, 3693.

[5] a) M. Maestri, N. Armaroli, V. Balzani, E. C. Constable, A. M. C. Cargill Thompson, *Inorg. Chem.* **1995**, *34*, 2759; b) A. El-ghayoury, A. Harriman, A. Khatyr, R. Ziessel, *Angew. Chem.* **2000**, *112*, 191; *Angew. Chem. Int. Ed.* **2000**, *39*, 185; c) M. Duatti, S. Tasca, F. C. Lynch, H. Bohlen, J. G. Vos, S. Stagni, M. D. Ward, *Inorg. Chem.* **2003**, *42*, 8377.

[6] a) R. Lieghio, P. G. Potvin, A. B. P. Lever, *Inorg. Chem.* **2001**, *40*, 5485; b) E. C. Constable, C. E. Housecroft, E. R. Schofield, S. Encinas, N. Armaroli, F. Barigelletti, L. Flamigni, E. Figgemeier, J. G. Vos, *Chem. Commun.* **1999**, 869; c) R. Ziessel, *Synthesis* **1999**, 1839.

[7] a) R. Passalacqua, F. Loiseau, S. Campagna, Y.-Q. Fang, G. S. Hanan, *Angew. Chem.* **2003**, *115*, 1649; *Angew. Chem. Int. Ed.* **2003**, *42*, 1608; b) Y.-Q. Fang, N. J. Taylor, G. S. Hanan, F. Loiseau, R. Passalacqua, S. Campagna, H. Nierengarten, A. Van Dorsselaer, *J. Am. Chem. Soc.* **2002**, *124*, 7912;

[8] A series of coplanar heterocyclic rings can be used to build up helical "foldamer" structures: a) G. S. Hanan, J.-M. Lehn, N. Kyritsakas, J. Fischer, *J. Chem. Soc. Chem. Commun.* **1995**, 765; b) G. S. Hanan, U. S. Schubert, D. Volkmer, E. Riviere, J.-M. Lehn, N. Kyritsakas, J. Fischer, *Can. J. Chem.* **1997**, *75*, 169; c) L. A. Cuccia, E. Ruiz, J.-M. Lehn, J.-C. Homo, M. Schmutz, *Chem. Eur. J.* **2002**, *8*, 3448, and references therein.

[9] K. O. Johansson, J. A. Lotoski, C. C. Tong, G. S. Hanan, *Chem. Commun.* **2000**, 819.

[10] F. Loiseau, R. Passalacqua, S. Campagna, M. I. J. Polson, Y.-Q. Fang, G. S. Hanan, *Photochem. Photobiol. Sci.* **2002**, *1*, 982.

[11] a) A. M. Garcia, D. M. Bassani, J.-M. Lehn, G. Baum, D. Fenske, *Chem. Eur. J.* **1999**, *5*, 1234; b) E. I. Lerner, S. J. Lippard, *Inorg. Chem.* **1977**, *16*, 1537.

[12] a) X. Chen, F. J. Femia, J. W. Babich, J. A. Zubieta, *Inorg. Chem.* **2001**, *40*, 2769; b) S. Chirayil, V. Hegde, Y. Jahng, R. P. Thummel, *Inorg. Chem.* **1991**, *30*, 2821; c) E. I. Lerner, S. J. Lippard, *J. Am. Chem. Soc.* **1976**, *98*, 5397.

[13] F. C. Schaefer, US 3294798, **1966**.

[14] M. I. J. Polson, N. J. Taylor, G. S. Hanan, *Chem. Commun.* **2002**, 1356.

[15] a) G. J. E. Davidson, S. J. Loeb, N. A. Parekh, J. A. Wisner, *J. Chem. Soc. Dalton Trans.* **2001**, 3135; b) E. C. Constable, C. E. Housecroft, M. Neuburger, D. Phillips, P. R. Raithby, E. Schofield, E. Sparr, D. A. Tocher, M. Zehnder, Y. Zimmermann, *J. Chem. Soc. Dalton Trans.* **2000**, 2219; c) E. C. Constable, E. Schofield, *Chem. Commun.* **1998**, 403.

[16] A. J. Downard, G. E. Honey, L. F. Phillips, P. J. Steel, *Inorg. Chem.* **1991**, *30*, 2259.

[17] a) G. S. Hanan, C. R. Arana, J.-M. Lehn, D. Fenske, *Angew. Chem.* **1995**, *107*, 1191; *Angew. Chem. Int. Ed. Engl.* **1995**, *34*, 1122; b) G. S. Hanan, C. R. Arana, J.-M. Lehn, G. Baum, D. Fenske, *Chem. Eur. J.* **1996**, *2*, 1292.

[18] D. K. Lavallee, E. B. Fleischer, *J. Am. Chem. Soc.* **1972**, *94*, 2583.

[19] R. P. Thummel, Y. Jahng, *Inorg. Chem.* **1986**, *25*, 2527.

[20] CCDC 181953 and 223934 contain the supplementary crystallographic data for this paper. These data can be obtained free of charge via www.ccdc.cam.ac.uk/conts/retrieving.html (or from the Cambridge Crystallographic Data Centre, 12 Union Road, Cambridge CB21EZ, UK; fax: (+44)1223-336-033; or deposit@ccdc.cam.uk).

[21] S. Pyo, E. Perez-Cordero, S. G. Bott, L. Echegoyen, *Inorg. Chem.* **1999**, *38*, 3337.

[22] a) C. M. Chamchoumis, P. G. Potvin, *J. Chem. Soc. Dalton Trans.* **1999**, 1373; b) K. L. Bushell, S. M. Couchman, J. C. Jeffery, L. H. Rees, M. D. Ward, *J. Chem. Soc. Dalton Trans.* **1998**, 3397; c) N. W. Alcock, P. R. Barker, J. M. Haider, M. J. Hannon, C. L. Painting, Z. Pikramenou, E. A. Plummer, K. Rissanen, P. Saarenketo, *J. Chem. Soc. Dalton Trans.* **2000**, 1447; d) B. Whittle, S. R. Batten, J. C. Jeffery, L. H. Rees, M. D. Ward, *J. Chem. Soc. Dalton Trans.* **1996**, 4249.

[23] M. Marcaccio, F. Paolucci, C. Paradisi, S. Roffia, C. Fontanesi, L. J. Yellowlees, S. Serroni, S. Campagna, G. Denti, V. Balzani, *J. Am. Chem. Soc.* **1999**, *121*, 10081, and references therein.

[24] Compound **3d** was previously synthesised, and its redox properties were briefly described. Reported data are in agreement with those obtained here: P. Paul, B. Tyagi, M. M. Bhadbhade, E. Suresh, *J. Chem. Soc. Dalton Trans.* **1997**, 2273.

[25] M. Beley, J.-P. Collin, J.-P. Sauvage, H. Sugihara, F. Heisel, A. Miehé, *J. Chem. Soc. Dalton Trans.* **1991**, 3157.

[26] G. R. Crosby, *Acc. Chem. Res.* **1975**, *8*, 231.

[27] K. Nakamoto, *J. Phys. Chem.* **1960**, *64*, 1420.

[28] C. Metcalfe, S. Spey, H. Adams, J. A. Thomas, *J. Chem. Soc. Dalton Trans.* **2002**, 4732.

[29] J. N. Demas, G. A. Crosby, *J. Phys. Chem.* **1971**, *75*, 991.

[30] N. Nakamaru, *Bull. Chem. Soc. Jpn.* **1982**, *55*, 2697.

[31] S. Campagna, G. Denti, S. Serroni, A. Juris, M. Venturi, V. Ricevuto, V. Balzani, *Chem. Eur. J.* **1995**, *1*, 211.

[32] F. H. Case, E. Koft, *J. Am. Chem. Soc.* **1959**, *81*, 905.

[33] B. P. Sullivan, J. M. Calvert, T. J. Meyer, *Inorg. Chem.* **1980**, *19*, 1404.